

Effect of Temperature on Carbon-Black Agglomeration in Hydrocarbon Liquid with Adsorbed Dispersant

You-Yeon Won,[†] Steve P. Meeker,[‡] Veronique Trappe,[§] and David A. Weitz^{*}

Department of Physics and DEAS, Harvard University, 29 Oxford Street, Cambridge, Massachusetts 02138

Nancy Z. Diggs and Jacob I. Emert

Infineum USA LP, Linden, New Jersey 07036

Received August 22, 2004. In Final Form: November 9, 2004

Suspensions of carbon black in oil, stabilized with adsorbed polyisobutylene succinimide (PIBSI) dispersant, are commonly used as model systems for investigating the soot-handling characteristics of motor oils. The structure of the carbon-black agglomerates changes dramatically with temperature; this results in a concomitant change in the suspension rheology. Linear and nonlinear rheological experiments indicate a large increase of the interparticle attractions as the temperature is raised. To elucidate the origin of this behavior, we investigate the effect of temperature on the stabilizing effect of the dispersant. Measurements of adsorption isotherms of the dispersant on carbon black indicate that there is little variation of the binding energy with temperature. Intrinsic viscosity measurements of PIBSI dispersants in solution clearly exhibit an inverse dependence of the dispersant chain dimension with temperature. These results suggest that the temperature-dependent changes in the chain conformation of the PIBSI dispersant are primarily responsible for the changes in the dispersion rheology, and we propose a simple model to account for these data.

1. Introduction

The effect of temperature on the stability of colloidal suspensions is important in many industrial applications. In particular, changes in particle interaction with temperature can significantly alter the physical properties of a colloidal dispersion. One industrially important system where temperature has an effect on the stabilization of colloidal particles and, hence, an enormous impact on flow properties is soot in used motor oil. Soot is a highly carbonaceous colloidal material produced as a byproduct of combustion in the engine. Some of the soot is retained in the engine oil, where the particles can agglomerate, increasing the viscosity of the oil and significantly diminishing its lubrication performance. The soot can also form a high-viscosity sludge which can also degrade lubricant effectiveness. To reduce this agglomeration, dispersants are added to the oil; these adsorb on the surface of the soot particles, thereby stabilizing them. A commonly used dispersant is a polyamine (PAM) with a polyisobutylene succinimide (PIBSI) tail; the PAM adsorbs on the surface of the soot, while the PIBSI tail provides steric stabilization. Because lubricants are required to function across a wide range of operating temperatures, the temperature dependence of the efficacy of the stabilization of the dispersant is a critical issue.

There is, in fact, a well-documented temperature dependence of the effect of soot dispersions on the viscosity of formulated engine oil; upon increasing temperature, the viscosity of the system can increase dramatically,¹ suggesting that soot attractions increase with tempera-

ture, even in the presence of the PIBSI dispersant. Although this phenomenon has been extensively investigated, its underlying origin is, as yet, unexplained. Three possible origins have been postulated: a temperature dependence of the adsorption of the dispersant on the surface of the soot, dispersant-mediated Coulombic charging of the soot, and a temperature dependence of the solvency of the dispersant molecules in the oil phase. In fact, the basic mechanism of the stabilization of soot is still unclear; both steric stabilization and charge stabilization have been suggested as possible mechanisms. Thus, a definitive study of the origin of the temperature dependence may also help establish the nature of the basic stabilization mechanism.

The first of the possible explanations is that the dispersant molecules desorb from the soot particles with increasing temperature, thereby allowing for more agglomeration of the soot. There have been contradictory reports of the temperature dependence of the adsorption, with both increases^{2–4} and decreases⁵ with increasing temperature having been reported. Typically, these experiments are performed using carbon black as a model for the soot, and the results depend on the surface chemistry of the carbon black that is used.

The second possible mechanism involves the role of charge in the stabilization of the soot. The role of charge in the stabilization of soot in nonpolar liquids is, in itself, still poorly understood, complicating a determination of the role of temperature on this mechanism. Measurements

^{*} To whom correspondence should be addressed. E-mail: weitz@deas.harvard.edu.

[†] Current address: School of Chemical Engineering, Purdue University, West Lafayette, IN 47907.

[‡] Current address: Rhodia, Aubervillier, Paris, France.

[§] Current address: Department of Physics, University of Fribourg, Switzerland.

(1) Selby, K. Society of Automotives Engineers Technical Paper No. 981369; Society of Automotives Engineers: Warrendale, PA, 1998.

(2) Dubois-Clochard, M.-C.; Durand, J.-P.; Delfort, B.; Gateau, P.; Barre, L.; Blanchard, I.; Chevalier, Y.; Gallo, R. *Langmuir* **2001**, *17*, 5901.

(3) Pugh, R. J.; Fowkes, F. M. *Colloids Surf.* **1984**, *9*, 33.

(4) Pugh, R. J.; Fowkes, F. M. *Colloids Surf.* **1984**, *11*, 423.

(5) Cox, A. R.; Mogford, R.; Vincent, B.; Harley, S. *Colloids Surf.*, **A** **2001**, *181*, 205.

of the zeta potential suggested that PIBSI dispersants can have two effects on soot; in addition to adsorbing on the surface of soot, they can also create charge exchange between the carbon surface and dispersant micelles in solution. This results in a charge on the surface of the soot which may also contribute to stabilization.⁶ This mechanism for stability is supported by calculation of the potential energy of interaction for sterically stabilized spherical particles; when the radius of the carbon particles exceeds about 200 nm, the distance of closest approach between particles caused by the steric barrier due to the dispersant coating, which is ~ 10 nm, becomes too short to sufficiently reduce the role of the van der Waals attractive forces.⁶ However, experiments with the same materials using a surface force apparatus to directly measure the forces between PIBSI-coated carbon surfaces showed that the repulsive effect has a short range of ~ 11 nm and that the measured pressure–distance profile is in quantitative agreement with an established polymer brush theory. This suggests that the electrostatic force is perhaps immeasurably weak and does not contribute to the stabilization.⁷ Moreover, such an electrostatic stabilization mechanism would not be expected to have a strong temperature dependence.⁸

The third proposed mechanism is the temperature dependence of the solubility of the PIBSI in the oil. In most cases, experiments indicate a robust correlation between the flocculation temperature of the colloidal particles and the theta (θ) temperature of the stabilizing polymer.⁸ The situation is more complicated in the case of PIBSI stabilization because changes in the temperature have two distinct consequences. First, an increase in the temperature may reduce the solvency of PIB in *n*-alkane; this is often referred to as the lower critical solution temperature or LCST phenomenon.^{9,10} Second, an increase in the temperature also affects the local conformation of the PIB chain itself.^{11–14} In both cases, the resultant effect is to shrink the moieties which provide the steric stabilization.

Clearly, a knowledge of how and why temperature affects the rheological properties of soot-loaded formulated engine oil is highly desirable. In this paper, we use a model system of carbon black in basestock oil and investigate the temperature dependence of the effectiveness of PIBSI in stabilizing the dispersion in an effort to understand the underlying mechanisms responsible for the stabilization of soot dispersions in used motor oil and the origin of its temperature dependence. We examine the temperature-dependent agglomerate structures of the carbon black and the resultant rheological properties of the suspensions. Application of the recently discovered scaling rules¹⁵ to the analyses of the linear and nonlinear rheology data allows us to quantitatively determine how the net interparticle attractions increase as the temperature is raised. We use Fourier transform infrared (FTIR) analyses of supernatants from carbon-black/PIBSI/oil samples to

investigate the temperature dependence of the amount of dispersant adsorbed on the carbon black and show that the degree of adsorption is independent of temperature. To investigate the effect of temperature on the steric stabilization induced by the dispersant, we measure the intrinsic viscosities of dispersant solutions to determine the size of the adsorbed steric barrier and show that the conformation of the PIBSI depends sensitively on temperature, with the size of the molecule decreasing with increasing temperature. These results are correlated with the measured temperature dependence of the rheological behavior of the carbon black, to determine the origin of the temperature dependence. We present a simple theoretical model that connects the independent experimental results. The combined results of our experiments and modeling suggest an important role of subtle changes in local chain conformation of the PIBSI dispersant on carbon-black destabilization.

2. Experimental Section

Materials. The carbon black used in this study is Vulcan XC72R, a high structure carbon black from Cabot Corp. The morphology of this material is defined on three levels: *primary particles* of about 30-nm diameter are fused together to form larger fractal clusters, ~ 500 nm in size, that cannot be broken, and which are often referred to as *primary aggregates*; in some cases, these primary aggregates form larger, more weakly bound *agglomerates*, for example, when dispersed in a hydrocarbon medium.¹⁵ The physicochemical characteristics of this carbon black including the specific surface area and porosity¹⁶ and surface chemical composition¹⁷ have been previously documented.

The dispersant studied was produced by condensation of polyisobutylene succinic anhydride, with a weight-average molecular weight $\bar{M}_w \approx 5000$ g/mol and a polydispersity of $\bar{M}_w/\bar{M}_n \approx 2.3$, where \bar{M}_n is the number-average molecular weight, and a branched poly(alkylene amine) (PAM), with $\bar{M}_n \approx 270$ g/mol. This dispersant can be considered as a short block copolymer with oleophilic PIB chains at the ends and a polar PAM segment in the middle. The overall molecular weight of the dispersant determined by gel permeation chromatography is $\bar{M}_w \approx 10\,000$ g/mol with a polydispersity of $\bar{M}_w/\bar{M}_n \approx 2.4$ and with an average of about 2.3 hydrocarbon (PIB) tails per molecule. We assume $R_g^2/\bar{M} \approx 0.570$ ($\text{\AA}^2 \cdot \text{mol}$)/g at 25 °C, where R_g is the radius of gyration and \bar{M} is the molecular weight, for linear PIB in the melt.¹⁸ Using the dispersant's effective \bar{M}_w to take branching into account,¹⁹ we estimate $R_g \approx 3.1$ nm on average for a dispersant in the random-walk configuration. The copolymer dispersant was received at an active ingredient level of 48.4 wt % in Exxon S150N basestock oil, and this solvent was used for all our rheology and adsorption experiments. In this paper, dispersant concentration is expressed as net active ingredient, rather than the concentration of the dispersant stock added.

Dispersions were prepared by adding the carbon black by weight to the basestock oil, mixing with a combination of vortexing for about 1 min, followed by ultrasonication at a power of ~ 140 W for 30 min. The samples were then slowly tumbled for at least 1 day at room temperature to ensure that the carbon black was well dispersed in the basestock oil. All samples with added dispersant were also equilibrated for at least 1 day by slow tumbling.

Rheology. Dynamic (oscillatory) and steady-shear rheology were used to investigate the structure and interactions in carbon-black suspensions as a function of temperature. Experiments were performed using a strain-controlled Rheometrics ARES rheometer which has a torque range of 0.004–100 g·cm in two ranges with 1% accuracy. We used a standard Couette cell that contained the sample in a 1-mm concentric cylindrical gap

(6) Pugh, R. J.; Matsunaga, T.; Fowkes, F. M. *Colloids Surf.* **1983**, *7*, 183.

(7) Georges, E.; Georges, J.-M.; Hollinger, S. *Langmuir* **1997**, *13*, 3454.

(8) Napper, D. H. *J. Colloid Interface Sci.* **1977**, *58*, 390.

(9) Patterson, D. *Macromolecules* **1969**, *2*, 672.

(10) Luna-Barcenas, G.; Gromov, D. G.; Meredith, J. C.; Sanchez, I. C.; de Pablo, J. J.; Johnston, K. P. *Chem. Phys. Lett.* **1997**, *278*, 302.

(11) Cifferi, A.; Hoeve, C. A. J.; Flory, P. J. *J. Am. Chem. Soc.* **1961**, *83*, 1015.

(12) Mark, J. E.; Thomas, G. B. *J. Phys. Chem.* **1966**, *70*, 3588.

(13) Suter, U. W.; Salz, E.; Flory, P. J. *Macromolecules* **1983**, *16*, 1317.

(14) DeBolt, L. C.; Suter, U. W. *Macromolecules* **1987**, *20*, 1425.

(15) Trappe, V.; Weitz, D. A. *Phys. Rev. Lett.* **2000**, *85*, 449.

(16) Cabot Corporation Home Page. <http://www.cabot-corp.com>.

(17) Clague, A. D. H.; Donnet, J. B.; Wang, T. K.; Peng, J. C. M. *Carbon* **1999**, *37*, 1553.

(18) Fetters, L. J.; Lohse, D. J.; Richter, D.; Witten, T. A.; Zirkel, A. *Macromolecules* **1994**, *27*, 4639.

(19) Zimm, B. H.; Stockmayer, W. H. *J. Chem. Phys.* **1949**, *17*, 1301.

between a cup, 34.0-mm diameter, and a bob, 32.0-mm diameter and 33.2 mm length. For the elastic gels of carbon black, the cup, which was the moving surface of the rheometer, was sand-blasted as a precautionary measure to mitigate possible slip of the sample at the surface. Temperature was controlled by a circulating ethylene glycol/water bath, typically to within ± 0.2 °C for the range probed, 5–100 °C.

When first loaded into the rheometer, each sample was presheared by applying a high steady shear stress on the order of 10^2 Pa for 10 min twice; this presumably breaks up all agglomerates greater than ~ 1 μm at room temperature, ensuring that the mixture begins as a dispersion of primary aggregates. This procedure was found to be essential to ensure reproducible results. Three types of dynamic tests were performed at each condition: (1) a linear dynamic time sweep at a frequency $\omega = 10$ rad/s to monitor the growth of the viscoelastic moduli over a time of 2000 s after the preshear as structure rebuilds in the sample, (2) a linear dynamic frequency sweep of the sample after this equilibration time, and (3) a dynamic strain amplitude sweep to ensure that the frequency sweep amplitude is in the linear regime, where the deformation is sufficiently small that the rheological response is independent of the strain amplitude. The range of linearity varies with sample concentration and temperature and, for carbon-black gels, is normally restricted to strain amplitudes below a few parts in 100. At each temperature, the samples were quiescently equilibrated for a minimum of 1 h before starting the sequence of tests. If necessary, between the tests, the bob was raised, and the sample was stirred for ~ 30 s, to ameliorate any possible effects of bulk sedimentation.

Measurements on the carbon-black dispersions under steady shear were performed at seven different shear rates ranging between 1750 and 0.1 s^{-1} . The suspension viscosities were measured as the shear rate was decreased in steps. At each shear rate, we sheared the sample at the set rate for 10 min prior to the measurement. Using this protocol, we obtained reproducible viscosity–shear-rate curves. Although we observed some effects of shear history dependence, long transients, and shear-induced structuring, these effects had little influence at high shear > 10 s^{-1} , while even at lower shear rates, the relative errors were estimated to be less than $\sim 20\%$.

Intrinsic Viscosity Measurements. To probe the temperature dependence of the intrinsic viscosity of the dispersant in basestock oil, we measured the viscosities of the solvent (η_0) and dispersant solutions (η) without carbon black at various dispersant concentrations (0.5, 1.0, 1.5, 2.0, and 3.0 wt %), each at two different temperatures, 40 and 100 °C. Measurements were done in a constant-temperature bath with an Ubbelohde capillary viscometer; we performed separate experiments to confirm that the dispersant solutions were Newtonian under all conditions. The measured viscosity data had experimental errors of at most a few tenths of a percent. Intrinsic viscosities of the dispersant, $[\eta]$, were determined two different ways: We used the extrapolated, zero-concentration values ($c \rightarrow 0$) of the reduced viscosities, $(\eta - \eta_0)/(\eta_0 c)$, using the Huggins equation for the virial expansion of the viscosity at low concentration,

$$\frac{\eta - \eta_0}{\eta_0 c} \approx [\eta] + k_H [\eta]^2 c \quad (2.1)$$

where k_H is the so-called Huggins coefficient.²⁰ We also determined the inherent viscosities, $\ln(\eta/\eta_0)/c$, again extrapolating to zero concentration, using the Kraemer equation for the virial expansion,

$$\frac{\ln(\eta/\eta_0)}{c} \approx [\eta] + \left(k_H - \frac{1}{2}\right) [\eta]^2 c \quad (2.2)$$

At each temperature, both the reduced and the inherent viscosities exhibited linear concentration dependences and had the same y intercept.

Adsorption Measurements. Two concentration regimes were investigated: 3.5 wt % carbon black with 0.1–0.6 wt %

total active dispersant for low surface coverages and 2.0 wt % carbon black with 0.5–6.0 wt % total active dispersant for higher surface coverage. After 1 day of equilibration under slow tumbling at room temperature, the solutions were filtered using 0.4- μm polycarbonate membranes (Corning) at a rate of ~ 1.0 mL/h to obtain approximately 4.0 mL of the carbon-black free dispersant phase. For adsorption at higher temperatures (50, 75, and 100 °C), the samples were first allowed to equilibrate in a controlled environment chamber (Type 19200, Thermolyne) at the desired temperature, which was controlled to ± 2 °C, for an additional 1–2 h after room-temperature equilibration. The samples were filtered at the elevated temperature. The free dispersant concentrations in the supernatant were determined by FTIR spectroscopy (Galaxy 3000, Mattson). Carbon-black solutions with no dispersant were used to obtain background signals, and the dispersant concentration was determined by means of the area under the peak at 1705 cm^{-1} , which corresponds to the dispersant's succinimide group. The data were analyzed by correlating the peak area with the concentration, determined from reference solutions with known dispersant concentrations within the range of 0.2–3.0 wt %. The absorption for all reference solutions obeyed the Beer–Lambert law. The amount of adsorbed dispersant was calculated from the difference between the free dispersant in the supernatant and the total dispersant added to the solution.

3. Results and Discussion

3.1. Effect of Temperature on Dispersion Structure and Rheology. We survey the structural and rheological properties of the carbon-black/dispersant/basestock-oil system over a wide range of temperatures and compositions. When dispersant is added, the structure of the carbon-black aggregates becomes very sensitive to variations in temperature. To illustrate this, agglomerate structures for 4.0 wt % carbon-black samples at two different temperatures, 25 and 100 °C, are recorded with optical microscopy as a function of dispersant concentration. The structure evolves from highly dispersed primary aggregates at high dispersant concentration to more strongly aggregated clusters as the dispersant concentration is decreased, to ultimately form a strongly connected gel network in the absence of dispersant. As shown in Figure 1, the temperature of the sample has a dramatic influence on this transition; increasing the temperature from 25 to 100 °C causes the transition to the gel state to occur at a significantly higher dispersant concentration. Clearly, the strength of the attractive interparticle interactions increases as the temperature is increased.

To elucidate the effect of temperature on the stability of the carbon black and on the interparticle interactions, we exploit the scaling behavior of frequency-dependent elastic, $G'(\omega)$, and viscous, $G''(\omega)$, moduli that has been observed for carbon black.^{15,21} For sufficiently large volume fractions, ϕ , of carbon black, the measured moduli for samples with different ϕ scale onto a single, universal master curve; this is accomplished by scaling both the magnitude and the frequency of each data set by the same factor. This scaling implies that the functional form of the modulus is the same, independent of ϕ . The scaling arises because the viscoelastic modulus has two contributions, one due to the viscosity of the solvent and the second due to the presence of a connected gel network formed by the carbon black. The contribution of the solvent is virtually independent of ϕ , while the contribution of the elastic network depends very strongly on the volume fraction of carbon black. Thus, effect of the carbon black can be characterized by its low-frequency plateau elastic modulus, G_p' , whose value can be determined from the scaling factor, even if it is too weak to be measured directly. These

(20) Rubinstein, M.; Colby, R. H. *Polymer Physics*; Oxford University Press: Oxford, 2003.

(21) Trappe, V.; Prasad, V.; Cipelletti, L.; Segre, P. N.; Weitz, D. A. *Nature* **2001**, *411*, 772.

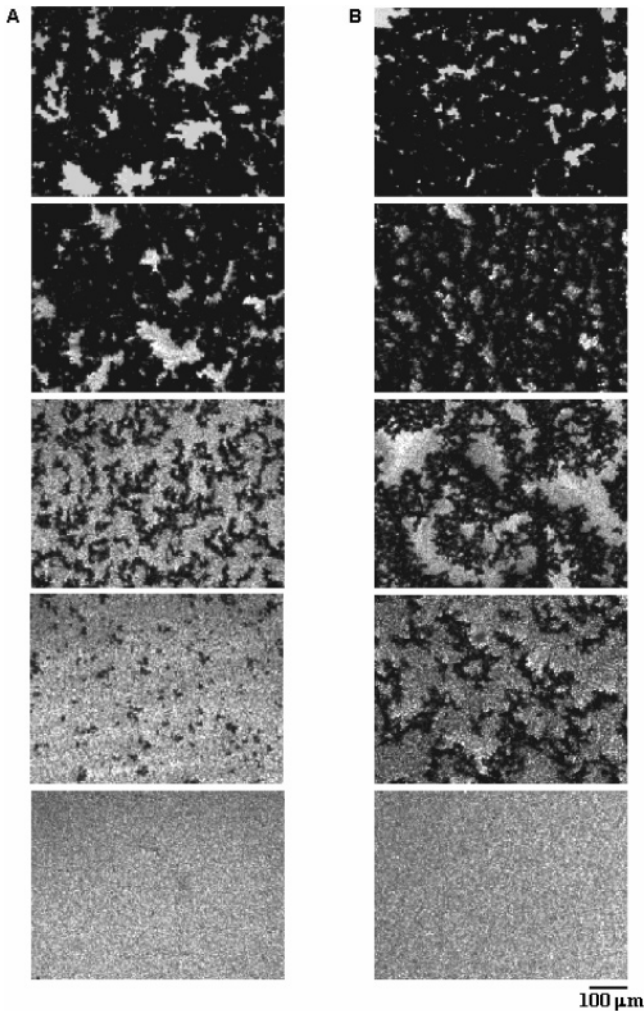


Figure 1. Optical micrographs of samples of 4.0 wt % carbon black at (A) 25 °C and (B) 100 °C showing the weakening network structure with either addition of dispersant or increasing temperature. The dispersant concentrations are (A) 0, 0.5, 0.7, 1.0, and 1.2 wt % and (B) 0, 0.5, 1.0, 1.5, and 1.9 wt % from top to bottom. All images were taken at the same magnification.

values of G_p' exhibit a critical behavior, scaling as $G_p' \sim (\phi - \phi_c)^{\nu_\phi}$, where ϕ_c is the critical value of the volume fraction where the sample first begins to exhibit a solidlike contribution to the viscoelastic response and $\nu_\phi \approx 4.1$. For lower volume fractions, below ϕ_c , the contribution of the carbon black is no longer that of a solid; instead, the viscosity of the suspension, as determined from the dynamic measurement of $G''(\omega)$, also exhibits a critical behavior, $\eta^* \sim (\phi_c - \phi)^{\nu_\phi}$, where $\nu_\phi \approx -0.13$.²¹ In both cases, the critical volume fraction for the onset of solidlike behavior is the same. Similar scaling is observed when the concentration of dispersant is varied; in this case, the fundamental variable is the strength of the attractive interaction between the particles, U .^{15,21,22} The data again scale onto the same universal master curve; G_p' exhibits a critical onset at a critical value of the interaction energy, U_c , and the viscosity exhibits a critical divergence at the same value of U_c . This behavior demonstrates that there is a critical volume fraction where the contribution of the carbon black to the viscoelastic response of the suspension becomes solidlike. Moreover, this value depends very sensitively on the strength of the attractive interaction

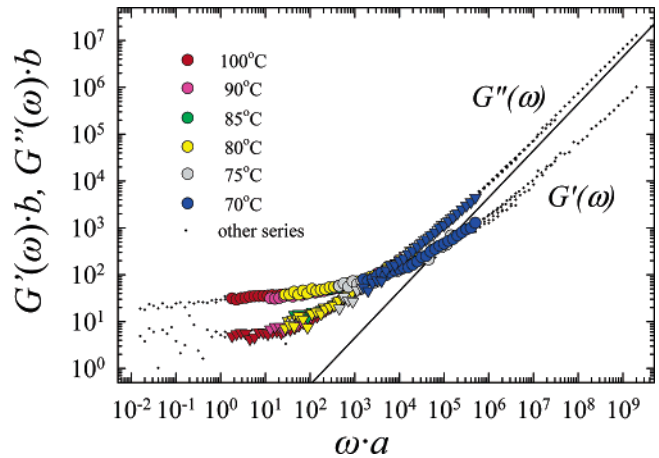


Figure 2. Master curve resulting from the scaling of the frequency-dependent elastic, $G'(\omega)$, and viscous, $G''(\omega)$, moduli as the temperature is varied. The linear dynamic responses were measured for a sample of 4.0 wt % carbon black at a dispersant concentration of 1.0 wt %. The solid line corresponds to the Newtonian viscosity of the oil. The data denoted as “other series” represent the scaled moduli for different carbon-black concentrations, ϕ , or interparticle interactions, U .¹⁵ Similar to the observations in the previous cases for variation in ϕ or U ,¹⁵ the linear relationship between the scaling factors, b and a/μ (where μ is the temperature-dependent solvent viscosity), was obeyed (data not shown).

between the primary aggregates of the carbon black, which, in turn, depends on the concentration of the dispersant. We emphasize, however, that the interaction energy should scale with temperature so that, within this picture, the effect of increasing temperature should be identical to decreasing the strength of the attractive interaction, which is the result of increasing the concentration of the dispersant.

To determine the effect of temperature on the linear viscoelastic properties of carbon-black suspensions, we measured $G'(\omega)$ and $G''(\omega)$ for a sample containing 4.0 wt % carbon black and 1.0 wt % dispersant at temperatures, T , ranging from 25 to 100 °C. The results are qualitatively different than expected from the simple scaling picture; at high temperatures, the sample is clearly an elastic solid, with $G'(\omega)$ nearly frequency independent and dominating $G''(\omega)$, whereas at low temperatures, the sample becomes fluidlike, with $G''(\omega)$ increasing linearly in ω and dominating $G'(\omega)$. Nevertheless, for sufficiently large T , the data can still be scaled onto the same master curve as the ϕ - and U -dependent data. This is shown in Figure 2, where the solid circles represent $G'(\omega)$ and the solid triangles represent $G''(\omega)$ measured as T is varied; for comparison, the smaller points represent the data that make up the master curve when ϕ and U are varied.

To quantify the effect of temperature, we determine the temperature dependence of G_p' from the scaling factors and plot the results as the squares in Figure 3A; the data exhibit an onset at a critical temperature of $T_c \approx 65$ °C. For temperatures below T_c , we measure the viscosity from the data, $\eta^* \equiv G^*/\omega$ where $G^* \equiv [(G')^2 + (G'')^2]^{1/2}$, and plot η^*/μ as a function of T as the triangles in Figure 3A, where we have normalized by the viscosity of the solvent with dispersant, to account for its temperature dependence. The data exhibit a divergence at a similar critical temperature. Surprisingly, both the plateau elastic modulus and the viscosity exhibit a critical scaling with temperature, with the viscosity scaling as $\eta^*/\mu \sim (T_c - T)^{\nu_T}$ with $\nu_T \approx -0.33$ as shown in Figure 3B and with the plateau modulus scaling as $G_p' \sim (T - T_c)^{\nu_T}$ with $\nu_T \approx 2.9$, as shown in Figure 3C. The value of the critical temper-

(22) Prasad, V.; Trappe, V.; Dinsmore, A. D.; Segre, P. N.; Cipelletti, L.; Weitz, D. A. *Faraday Discuss.* **2003**, *123*, 1.

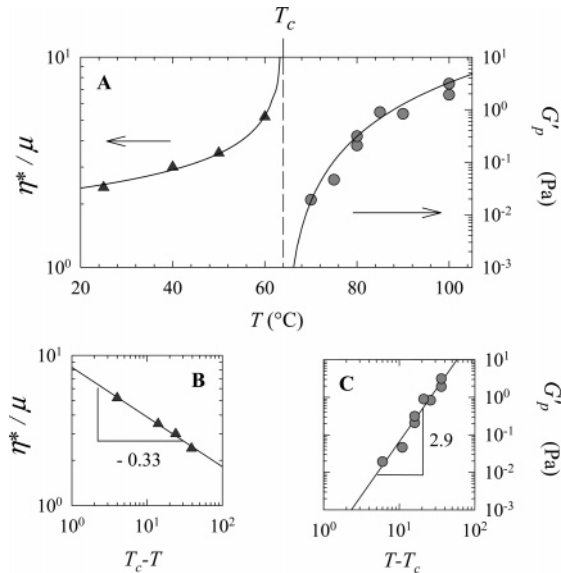


Figure 3. Results from analyses of the rheology data for the 4.0 wt % carbon black and 1.0 dispersant sample (Figure 2). The dependences on temperature, T , of the plateau modulus, G_p' , of the gels and the solvent-scaled complex viscosity (η^*/μ) from the fluid phases exhibit critical-like behavior, demonstrated in the lower panels. The solid curves in the upper panel were constructed on the basis of the best fit parameters for $G_p' \sim (T - T_c)^{\nu_T}$ and $\eta^* \sim (T_c - T)^{\nu_T}$. The resultant fit values are $T_c \approx 65$ °C, $\nu_T \approx 3$, and $\nu_T \approx -0.3$.

ature is the same in both cases, $T_c \approx 65$ °C. Thus, these data demonstrate that there is a critical onset to solidlike behavior that occurs at T_c . This behavior is reminiscent of that expected for a change in interaction energy between the primary aggregates of the carbon black; we emphasize, however, that this behavior cannot reflect the same sort of dependence on temperature, because the strength of the interaction exhibits an increase with temperature rather than the decrease that would be expected.

Further insight is obtained by studying the same sample when a steady shear is applied. We measure viscosity as a function of shear rate, $\dot{\gamma}$, from 1750 to 0.1 s^{-1} at temperatures both above and below T_c and plot the resultant relative viscosity, η/μ , as a function of $\dot{\gamma}$ in Figure 4A. At all temperatures, the data exhibit shear thinning, even below T_c , when the suspension is fluidlike. Thus, the carbon-black particles tend to form structures larger than primary aggregates at all temperatures. Just as for the linear viscoelasticity, an increase in the interaction energy between particles upon heating was apparent in the increased relative viscosity and enhanced degree of shear thinning. The nonlinear rheological behavior of carbon-black suspensions can also be scaled onto a single master curve for different particle volume fractions and different dispersant concentrations; this is accomplished by independently scaling both the stress and the shear rate for each data set.¹⁵ Similar scaling behavior is observed for the nonlinear data for different temperatures; however, only $\dot{\gamma}$, and not η/μ , must be scaled by a factor, a , to produce the master curve, shown in Figure 4B. The data superpose well over an extended range of shear rates, with the exception of the few scattered data points at the lowest reduced shear rates, $\dot{\gamma}a < 0.02$ s^{-1} , where the measured data have larger errors due to effects such as longer transients. Nevertheless, the scaling of the data can be used to quantitatively determine the effect of temperature on the pairwise interactions between the carbon-black particles. This is accomplished by recognizing that, at high shear rates, the resultant viscous stresses of the solvent

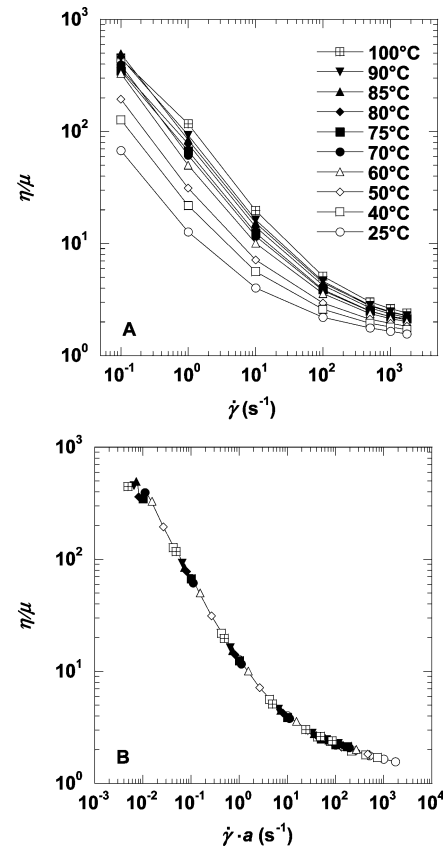


Figure 4. (A) Dependence of the viscosity, η , on shear rate, $\dot{\gamma}$, for a 4.0 wt % carbon-black suspension with 1.0 wt % added dispersant, as a function of temperature. The data presented have been normalized with the temperature-dependent viscosity of the dispersant solution in oil, μ , to compare the flow behavior. (B) Scaling behavior of the shear-rate-dependent viscosity measured at various temperatures. A master curve showing the scaled relative viscosity, η/μ , as a function of the scaled shear rate, $\dot{\gamma}a$, is constructed using the reference temperature $T = 25$ °C by shifting horizontally the data from part A.

on the carbon-black agglomerates are sufficient to fully break them apart so that only the primary aggregates remain. The stress required to do this is given by the stress when the viscosity data first begin to increase as $\dot{\gamma}$ is decreased from its maximum value. While the precise value of the shear stress cannot be determined exactly, the temperature dependence of this stress can be determined directly from the temperature dependence of the scaling parameters, a . This provides a direct measure of the temperature dependence of the interaction strength between primary aggregates of carbon black.

The behavior of G_p' provides a direct method of quantitatively investigating the role of the dispersant on the temperature dependence of the stability of the carbon black. We note, however, that while the transition between fluidlike and solidlike behaviors of the carbon black is a convenient demarcation to indicate a change in properties, agglomeration of the primary aggregates still occurs even if the carbon black does not form a connected network; it is only when the particles are fully dispersed that there is minimal impact on the rheological properties of the suspension. However, to quantitatively investigate the effects of the temperature dependence, we use G_p' as a probe of the relative stability of the carbon black.

To further explore the mechanism responsible for the temperature dependence of the stability, we investigate the behavior of G_p' at four different dispersant concentrations. With no dispersant added, the rheology of the carbon-

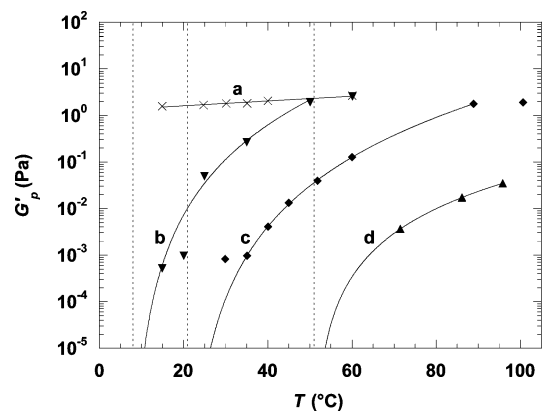


Figure 5. Correlation between G_p' and T as a function of dispersant concentration for samples of 2.0 wt % carbon black; the dispersant concentrations are (a) 0, (b) 0.1, (c) 0.2, and (d) 0.3 wt %. For samples with added dispersant, the measured T_c values are about (b) 8, (c) 21, and (d) 51 °C. Solid lines are guides to the eye.

black suspension is only slightly susceptible to temperature changes. Heating a 2.0 wt % carbon-black sample with no dispersant from 15 to 60 °C results in a very small, but still measurable, increase in G_p' , from 1.6 to 2.7 Pa, as shown by the \times symbols in Figure 5. By contrast, in the presence of dispersant, the system becomes significantly more temperature-dependent, as revealed by the results obtained at dispersant concentrations of 0.1, 0.2, and 0.3 wt %. In each case, as the temperature is raised, the dispersant becomes increasingly less effective in reducing the interparticle interactions and thereby reducing G_p' . The temperature of the resultant fluid–gel transition is strongly influenced by the concentration of dispersant; T_c increases from ~ 8 °C for 0.1 wt % dispersant to 21 °C for 0.2 wt % dispersant and to 51 °C for 0.3 wt % dispersant, as shown by the solid points in Figure 5. These results clearly indicate that the temperature-induced increase in G_p' and the commensurate enhancement in gelation are consequences of the stabilizing effect of the dispersant rather than a temperature dependence of the intrinsic carbon-black interparticle attraction.

3.2. Effect of Temperature on Dispersant Adsorption. One possible simple explanation for the observed behavior is that the adsorption of the dispersant on the surface of the carbon black is temperature-dependent and that, as the temperature increases, the amount of adsorption decreases, thereby resulting in a reduced stability of the particles. To investigate this possibility, the adsorption properties of the dispersant are evaluated at various temperatures using FTIR to measure the amount of dispersant in the supernatant, after the carbon black and adsorbed dispersant are filtered from the suspension. A typical example of the data obtained is illustrated by the measured FTIR absorbance near 1705 cm^{-1} of the supernatant of a sample with 3.5 wt % carbon black and 0.2 wt % dispersant for temperatures of 25, 50, and 100 °C, shown by the points in Figure 6A. There is clearly no change whatsoever in the absorbance with sample temperature. By comparison, the absorbance of a sample with the same dispersant concentration, but with no added carbon black, is shown by the solid line in Figure 6A; the difference in absorbance indicates the degree of adsorption of the dispersant on the surface of the carbon-black particles. Similar measurements were obtained for other initial concentrations of dispersant.

We summarize the results of the temperature-dependence adsorption in the isotherms shown in Figure 6B, where we plot the dependence of the adsorbed

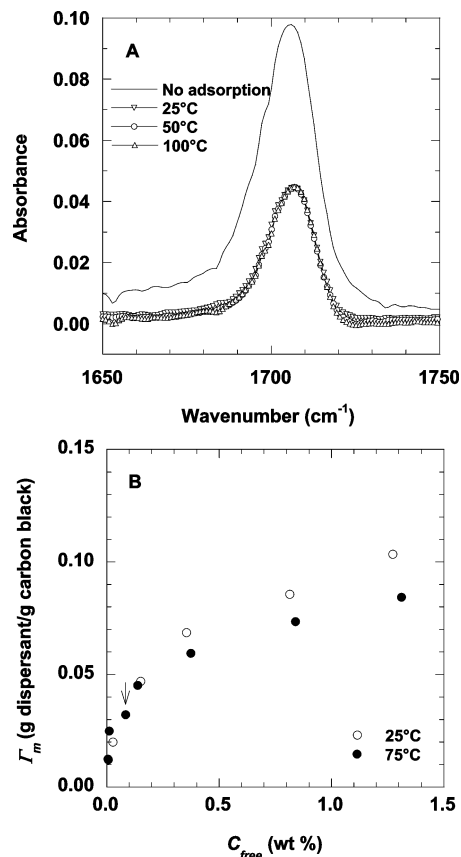


Figure 6. (A) Infrared absorbance spectra obtained from the free dispersant phases at equilibrium at four temperatures, demonstrating that there is no temperature dependence of the adsorption. (B) Dispersant-carbon-black adsorption isotherms at 25 and 75 °C. No significant desorption is observed with increasing temperature. The equilibration time was about 1–2 h. The arrow refers to the unbound dispersant concentration (i.e., $C_{\text{eq}} \approx 0.08$ wt %) at which the data in part A were taken.

concentration, Γ_m , as a function of free dispersant concentration in solution, C_{free} , for two temperatures, 25 and 75 °C, obtained using 3.5 and 2.0 wt % carbon-black samples. The observed behavior is consistent with that previously reported for PIBSI-based dispersants.^{2,4,5} At low concentrations of free dispersant, $C_{\text{free}} < 0.2$ wt %, the adsorption isotherms increase linearly, as expected for Langmuir adsorption kinetics in the dilute limit; however, the y intercept is nonzero, indicating some level of irreversible adsorption, presumably due to the binding of the dispersant's amine group to the polar (nitrogen or oxygen) sites of the carbon-black surface.¹⁷ At higher free dispersant concentrations, the rate of increase of Γ_m becomes more gradual, with the crossover to this regime occurring for $C_{\text{free}} \approx 0.2$ – 0.3 wt %. However, the adsorbed amount neither reaches a complete plateau, indicating surface saturation, nor exhibits a sudden upturn at high adsorption due to multilayer or surface-aggregate formation.^{2,5,23}

As illustrated for the data for 25 and 75 °C in Figure 6B, the qualitative features of the adsorption isotherms vary very little with temperature. At the highest dispersant concentrations ($C_{\text{free}} > 0.3$ wt %), the adsorption decreases very slightly, by about 18%, with increasing temperature. However, at the low surface coverage regime, $C_{\text{free}} < 0.2$ wt %, where the temperature-driven fluid–gel transition is normally observed, no change in the adsorbed

(23) Tomlinson, A.; Scherer, B.; Karakosta, E.; Oakey, M.; Danks, T. N.; Heyes, D. M.; Taylor, S. E. *Carbon* **2000**, *38*, 13.

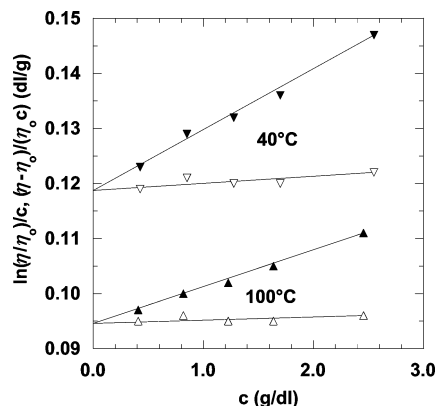


Figure 7. Reduced viscosity, $(\eta - \eta_0)/(\eta_0 c)$ (filled symbols), and inherent viscosity, $\ln(\eta/\eta_0)/c$ (open symbols), as functions of dispersant concentration, c , at 40 °C (downward triangles) and 100 °C (upward triangles). The intrinsic viscosity, $[\eta]$, is determined by the common intercepts at $c = 0$ of the reduced and inherent viscosities, using eqs 2.1 and 2.2. The solid lines represent the corresponding fits to the experimental data for the determination of $[\eta]$.

amount is detected upon increased temperature. Thus, the temperature dependence of the stability of carbon black is not a result of variations in the degree of adsorption of the dispersant.

3.3. Effect of Temperature on Dispersant Chain Conformation. The remaining possibility to account for the anomalous temperature dependence of the stability of the carbon black is the reduced effectiveness of the adsorbed dispersant due to temperature-dependent changes in the conformation of its PIB tails. Thermally induced PIB chain collapse in organic solvents has long been recognized; at elevated temperatures, the steric strain that restricts the local rotational isomeric states of the PIB segments is relieved, and the PIB chain becomes more kinked, resulting in a decrease in the dimensions of the chain.^{11–13} At temperatures that approach the LCST of a PIB solution, a similar chain collapse is observed, associated with the phase transition behavior.^{9,10} To investigate this possibility, we measured the intrinsic viscosity of solutions of dispersant in basestock oil at two different temperatures, 40 and 100 °C.

We restricted our investigation to systems consisting of dispersant and oil; we assume that the temperature behavior of adsorbed dispersant at the particle surfaces has the same temperature dependence. On the basis of an uncertainty of about 0.2% in our viscosity measurements, we used dispersant concentrations between 0.5 and 3.0 wt % to reliably determine the dependences of the reduced viscosity, $(\eta - \eta_0)/(\eta_0 c)$, and the inherent viscosity, $\ln(\eta/\eta_0)/c$, on dispersant concentration, c . In this range of concentration, both the reduced and the inherent viscosities vary linearly with c and both extrapolate to the same intercept at zero concentration, as expected from the Huggins and Kraemer relations, eqs 2.1 and 2.2, respectively. The data for the intrinsic viscosity, $[\eta]$, were determined from the y intercepts of the linear fits of the data to both the Huggins and the Kraemer equations, as shown in Figure 7. The resultant $[\eta]$ values show a significant decrease as temperature increases. Using the relations $[\eta] \sim R_g^2 R_h / \bar{M}$ and $R_h \sim R_g$, where R_h is the hydrodynamic radius,^{24,25} we can estimate that, for example, heating the sample from 40 to 100 °C results in

a decrease of about 7% in the average hydrodynamic radius for the dispersant-free chains. Thus, the dispersants adopt more collapsed conformations at higher temperatures, presumably as a result of the local chain conformational effects and/or the decreased PIB solvency. We emphasize that we detected no evidence of dispersant phase separation, such as optical heterogeneity, in any of the samples studied.

3.4. Consistency between Dispersant Collapse and Dispersion Rheology. To ascertain that the temperature dependence of the conformation of the adsorbed dispersant is the origin of the changes in carbon-black stability, we estimate the role of the change of the conformation on the interparticle interaction and compare this with the measurements using the shear-rate dependence. We use the experimental measurements of the intrinsic viscosity as a basis of a model that determines how temperature changes of the dispersant conformation affect the pair interaction potential between dispersant-coated carbon-black particles. We assume that the effect of the adsorbed polymer brushes of thickness, L , is simply to increase the distance of closest approach between the particles to $D \approx 2L$ and, thus, to weaken the role of the van der Waals attraction.²⁶ The strength of the attractive-pair-interaction energy, U , between two dispersant-coated carbon-black particles can, to a reasonable approximation, be described as a sum of the van der Waals attraction, U_{vdW} , between the core particles and a hard-wall-like repulsion between the adsorbed films upon overlap. This allows us to estimate the interaction potential between two particles.

We note that the difference in dielectric properties between the stabilizing PIB moieties and the hydrocarbon medium, which is the fundamental driving force for the polymeric van der Waals contribution,²⁷ is not significant; on the basis of the measured refractive indices of $n_{\text{PIB}} \approx 1.510$ and $n_{\text{oil}} \approx 1.476$ at room temperature, we expect that even complete collapse of the adsorbed PIB would cause the polymeric continuum van der Waals contributions to become only a fraction of $k_B T$. Therefore, it is unlikely that a van der Waals attraction between the steric PIB layers is a possible source of the observed colloidal gelation occurring at high temperatures.

At separation distances between dispersant-coated particles comparable to the distances where the adsorbed brushes overlap, the retardation of the van der Waals interactions between the core particles is not negligible. Thus, we use the Derjaguin approximation within the Lifshitz theory²⁸ and calculate the retarded attraction between identical graphite spheres of radius R_p ,

$$U_{\text{vdW}}(D) \approx -\frac{R_p}{12} \int_D^{\infty} \frac{A_{121}(x)}{x^2} dx \quad (3.1)$$

where A_{121} is the Hamaker function. In applying this model to the highly open structure of the carbon black, we use the primary particle size rather than some effective primary aggregate size, because it is the primary particles themselves that constitute the peripheries of the primary aggregates and that primarily control the interparticle forces.²⁹ As a result of the additional contributions to the attraction from the structures that exist around a single primary particle, the use of the primary particle radius leads to underestimation of the interaction potential;

(24) Weill, G.; des Cloizeaux, J. *J. Phys. (Paris)* **1979**, *40*, 99.
 (25) Wang, S.-Q.; Douglas, J. F.; Freed, K. F. *J. Chem. Phys.* **1987**, *87*, 1346.

(26) Bevan, M. A.; Prieve, D. C. *Langmuir* **2000**, *16*, 9274.
 (27) Parsegian, V. A. *J. Colloid Interface Sci.* **1975**, *51*, 543.
 (28) Hough, D. B.; White, L. R. *Adv. Colloid Interface Sci.* **1980**, *14*, 3.
 (29) Parfitt, G. D.; Picton, N. H. *Trans. Faraday Soc.* **1968**, *64*, 1955.

however, the associated temperature dependence of U_{vdW} is not sensitive to this assumption. To calculate $A_{121}(x)$, we use a methodology developed for the dispersion relations for anisotropic graphite half spaces separated by a liquid medium and the dielectric spectra of graphite.³⁰ The frequency-dependent dielectric response of oil is estimated using the damped-harmonic-oscillator model with constant values that are calculated from published data for *n*-hexadecane, with a correction for the density difference between oil and *n*-hexadecane estimated using Clausius–Mossotti theory.²⁸ The temperature dependence of $A_{121}(x)$ is taken into account by estimating the change in the dielectric spectrum of oil with temperature³¹ from the estimated change in the density of the oil³² and assuming no change in the dielectric properties of the solid carbon black. Thus, there are no adjustable parameters used in the calculation.

To calculate the separation distances for steric hard-wall repulsion, $D \approx 2L$, we define the brush height, L , as the second moment of the brush segment density profile. To estimate the values of L as a function of T , we first determine the temperature-dependent conformational properties of the dispersant chain in terms of the ratio R_g^2/\bar{M} , which is a measure of the backbone stiffness. We use the measured temperature dependence of the intrinsic viscosity in oil, $d \ln[\eta]/dT \approx -3.8 \times 10^{-3} \text{ (K}^{-1}\text{)}$, assuming that the dispersant chains are Gaussian, with $R_g^2/\bar{M} \approx 0.095 \text{ (\AA}^2\cdot\text{mol)/g}$ at 25 °C,¹⁸ similar to the homopolymer PIB.³³ Using surface grafting densities of the PIB arms estimated from the adsorption measurements, we obtain realistic estimates of L for spherical brushes using an established self-consistent field model.³⁴ In a sample of 4.0 wt % carbon black plus 1.0 wt % dispersant, for example, the dispersant layer thickness is estimated to monotonically decrease between 5.0 and 5.7 nm as the temperature is raised from 25 to 100 °C. These calculated values are comparable to the temperature-dependent end-to-end distances of the PIB arm with $\bar{M}_w \approx 5000 \text{ g/mol}$ in a random-walk configuration.

These models for the distance dependence of the van der Waals attraction, $U_{\text{vdW}}(D)$, and the brush separation, L , enable us to estimate theoretically the temperature dependence of the strength of attraction between two primary aggregates of carbon black. To estimate the temperature-dependent attractive force between primary aggregates, $F(T)$, we use the first derivative of the potential evaluated at the distance of contact; however, because the full interaction potential is the sum of two terms, the derivative is strictly not defined at the minimum, where the contribution of each term is equal. Thus, instead, we approximate the bonding force by the derivative of the van der Waals contribution, $F \approx U_{\text{vdW}}'(2L)$, where the prime represents the derivative with respect to distance, D , and we evaluate this at the point of contact, $2L$. Thus, we can calculate the expected temperature dependence of the binding force between primary aggregates, which we express as a ratio normalized to the value at 25 °C, $F(T)/F(T = 25 \text{ °C})$. This behavior is shown by the open circles in Figure 8.

For comparison, we can also experimentally determine the temperature dependence of the interparticle interac-

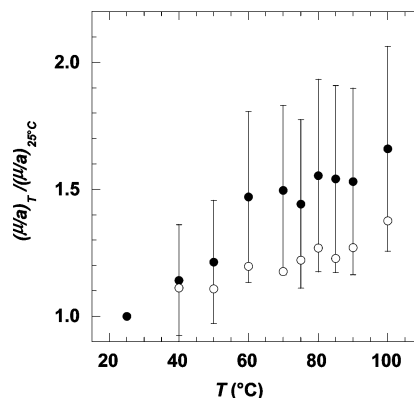


Figure 8. Temperature dependence of $(\mu a)_T/(\mu a)_{25^\circ\text{C}}$ (filled circles) determined from the applied shifts in scaling the steady-shear viscosities measured as functions of $\dot{\gamma}$ using a sample of the 4.0 wt % carbon black and 1.0 wt % dispersant (from Figure 4). The results are determined from the scale factors used to create the master curve. The error bars represent the uncertainties associated with the rheological experiments. They are compared to the predictions for $F(T)/F(T = 25^\circ\text{C})$, where $F = U_{\text{vdW}}(2L)$, shown by the open circles.

tion. We assume that the force required to break up the aggregates is caused by the viscous drag on them in the shear flow and is given by $(5/2)\pi\mu\dot{\gamma}R_h^2$.³⁵ We can estimate the temperature dependence of this quantity from our data for the shear-rate dependence of the viscosity of the solution. The shear rate where the viscosity just begins to increase presumably reflects the shear stress required to break the agglomerates completely and, thus, to break the bond between two primary aggregates. Rather than determine this empirically from the shape of the data, we instead take advantage of the scaling of the data and use the ratio μ/a , where μ accounts for temperature dependence of the viscosity of the oil with dispersant and a is the shear-rate shift factor obtained from the scaling. We again normalize the data to the value at 25 °C and determine the values of $(\mu/a)_T/(\mu/a)_{25^\circ\text{C}}$ for a sample of 4.0 wt % carbon black and 1.0 wt % dispersant for temperatures from 25 to 100 °C. We plot these values as solid points in Figure 8; they are in good accord with the theoretical predictions.

We make several assumptions and approximations in making our theoretical estimates. Nevertheless, the agreement between the calculation and the experimental measure of the interaction potential is very good. This provides strong evidence to support the hypothesis that the origin of the stability of carbon black is the steric interaction due to the adsorbed dispersant. Moreover, the temperature dependence of the stability results from the changes in the conformation of the dispersant tails as a function of temperature. This is most likely also the origin of the temperature dependence of the soot-induced changes in the viscosity in used motor oil.

4. Summary

The structure of the carbon-black aggregates and the resultant suspension rheology change dramatically as the temperature of the sample is increased. At low temperatures the primary aggregates are separate and well-dispersed, and fluidlike rheology is observed for the suspension. By contrast, at high temperatures the primary aggregates agglomerate, forming a more tenuous, sample-spanning network resulting in a solidlike rheology for the suspension. The interparticle attractive interactions

(30) Dagastine, R. R.; Prieve, D. C.; White, L. R. *J. Colloid Interface Sci.* **2002**, *249*, 78.

(31) Dagastine, R. R.; Prieve, D. C.; White, L. R. *J. Colloid Interface Sci.* **2000**, *231*, 351.

(32) Meerwall, E. v.; Beckman, S.; Jang, J.; Mattice, W. L. *J. Chem. Phys.* **1998**, *108*, 4299.

(33) Krigbaum, W. R.; Flory, P. J. *J. Polym. Sci.* **1953**, *9*, 37.

(34) Dan, N.; Tirrell, M. *Macromolecules* **1992**, *25*, 2890.

(35) Goldsmith, H. I.; Mason, S. G. In *Rheology: Theory and Applications*; Eirich, F. R., Ed.; Academic Press: New York, 1967.

increase as the temperature is raised, resulting in a critical-like fluid-to-gel transition. We investigate the effects of temperature on the repulsive portion of the interparticle interaction potential due to the steric stabilization of the dispersant as well as the attractive interaction resulting from the van der Waals forces.

Determination of the adsorption isotherms of dispersant on carbon black, made by FTIR measurements of the free dispersant concentration, indicates that the adsorption of the dispersant does not vary with temperature. Moreover, rheological measurements of a carbon-black sample without added dispersant shows virtually no temperature dependence; thus, it is unlikely that heating induces a significant increase in the van der Waals interaction between the carbon-black particles. Instead, the temperature-dependent intrinsic viscosity of the dispersant suggests that increasing temperature causes conformational changes in the hydrocarbon chain of the dispersant, causing it to collapse, thereby decreasing its efficiency in inhibiting agglomeration. We present theoretical estimates of the temperature dependence of the pair interaction energy and compare these with estimates of the temperature dependence of the stress required to break

the bond between primary aggregates which are determined from the observed scaling of the viscosity as a function of shear rate. We find good agreement between the theoretical and experimental estimates.

Our results suggest that steric repulsion due to the adsorbed dispersant is the dominant mechanism stabilizing the carbon black in the oil. Moreover, they suggest that the temperature dependence of the conformation of the tails of the adsorbed dispersant is the origin of the anomalous temperature dependence of the stability of carbon black. These results also suggest that the same mechanisms are responsible for both the stability of soot in used motor oil and the temperature dependence of this stability. The temperature dependence of this stability is technologically important, and the reduction in dispersancy at high temperatures must be considered in the design of motor oil additives.

Acknowledgment. The authors wish to thank Infineum for funding and for permission to publish these results.

LA047906T